

05,06,07

Modification of the electronic structure of the magnetic semiconductor surface with a strong Rashba effect caused by the presence of domain walls

© V.N. Men'shov^{1,2,3}, I.P. Rusinov^{1,2}, E.V. Chulkov²

¹ Lebedev Physical Institute, Russian Academy of Sciences, Moscow, Russia

² St. Petersburg State University, St. Petersburg, Russia

³ National Research Center „Kurchatov Institute“, Moscow, Russia

E-mail: v.menshov@lebedev.ru

Received July 1, 2025

Revised July 14, 2025

Accepted July 14, 2025

In this paper, we theoretically study how electron scattering on domain walls modifies the surface electronic structure of a magnetic semiconductor with a strong Rashba effect. It is shown that a smooth boundary between domains with opposite magnetization perpendicular to the surface induces the appearance of three different types of one-dimensional electronic states. A bound state is formed below the continuum of two-dimensional states. A resonant state with a quasi-linear spectrum and resonant states with a parabolic dispersion arise within the local energy exchange gap. The origin of the resonant states is related to the nontrivial Berry curvature due to the inversion symmetry breaking at the surface. The spectral characteristics and spin polarization of these states are described as a function of the Rashba splitting strength, the magnetization amplitude in the domains and the width of the boundary between them. The possible manifestation of the resonant states in magnetotransport experiments, for example, on the surface of the BiTeI polar semiconductor doped with transition metal atoms is discussed.

Keywords: Rashba effect, magnetic domain wall, exchange gap, resonant state.

DOI: 10.61011/PSS.2025.08.62261.173-25

1. Introduction

Today, on the basis of Van der Waals materials that combine a strong spin-orbit coupling (SOC) with a magnetic order and heterostructure based on these materials, a lot of various platforms are proposed for implementing and investigating new phenomena, among which a quantum anomalous Hall effect (AHE) [1–3] and a magnetoelectric effect in the axion insulator phase are prominent [4,5]. The explanation of these effects is rooted in a Berry curvature concept of the system states in a momentum space, which is pivotal in a solid-state topology theory [6,7]. The Chern number C , which is determined by the Berry curvature integral over filled states, characterizes the intrinsic AHE in the two-dimensional (2D) magnetic [1,2]. In an ideal situation, when a film of the magnetic topological insulator (TI) is in a single-domain state, transport (when the Fermi level is fixed in an energy gap) is carried out via a nondissipative chiral edge state localized along the sample perimeter, which is materialized in quantized transverse conductivity $\sigma_{xy} = Ce^2/h$ and no longitudinal conductivity $\sigma_{xx} = 0$, where $|C| = 1$ [1,2]. A sign of the topological invariant C and chirality are associated to a direction of the magnetization component that is normal to the film. However, fluctuations of the magnetic order are unavoidable in a real material. As a result, magnetization of the sample

obtains a multi-domain texture during remagnetization in an external field. This process in the TI ultrathin film with the intrinsic or impurity magnetic order is accompanied by appearance of a random net of conducting channels along the boundaries between the oppositely-polarized magnetic domains, which at the same time are topological boundaries. That is why the one-dimensional (1D) electron state induced by a magnetic domain wall (DW) as well as an edge state is commonly referred to as a topologically protected one [8,9].

Existence of chiral channels with quantum conductance on the domain walls and their contribution to transport properties of the magnetic topological insulators is confirmed by experimental data [8–11]. As an example, we can refer to such effects as drop of magnetoresistance with increase of concentration of the domain walls in an area of the coercive field [8] and a percolation nature of topological transitions, which are induced by the external field, between phases of the quantum AHE and the axion insulator or the trivial insulator [12]. It indicates that the charge transport in the magnetic topological insulators is related to distribution of magnetization in the sample through a network of the conducting channels, which implies an intricate and rich physics of the phenomenon. The electron states on the magnetic domain walls in the topological insulators were theoretically studied in some studies [13–22].

Interest to materials and systems with topological specific features of a band structure and to low-dimensional electron states on the structural and phase boundaries in them is not limited to the magnetic topological insulators [23]. However, very little attention is paid to surface states in the magnetic semiconductors with the strong SOC. Spectroscopic measurements and *ab initio* calculations of the BiTeI polar semiconductor show gigantic Rashba splitting of the surface states [24–26]. The authors [27–29] have found that doping the BiTeI samples with V or Mn atoms resulted in formation of a ferromagnetic order with a quite high Curie temperature on their surface. This phenomenon is explained as a result of indirect interaction of impurity magnetic moments via Rashba-type 2D states [29]. Besides, it was found that the magnetic order in the Rashba-effect diluted magnetic semiconductor (REMS) had a multi-domain structure [28]. Unfortunately, there are still no reports on studying magnetic transport properties in the $\text{Bi}_{1-x}(\text{V},\text{Mn})_x\text{TeI}$ material.

It has been recently shown that the hard domain wall results in appearance of a resonant state with linear dispersion in the energy interval of the local exchange gap on the REMS surface [30]. With weak exchange splitting relative to the Rashba splitting this state is quite stable and spin-polarized. By taking into account unique properties of the resonant state, it was predicted in the study [31] that the magnetic texture that consists of a pair of parallel domain walls could realize the almost semi-quantized anomalous Hall effect with $|\sigma_{xy}| = e^2/2h$ on the REMS surface.

In the present article, we study the electron states on the surface of the diluted magnetic semiconductor with strong Rashba splitting and spatially inhomogeneous magnetization. We consider a situation when the impurity magnetic moments are ordered orthogonally to the surface, but it is assumed that the domain wall exists. It is shown that 1D states of the various type can appear at a solitary boundary between the domains with oppositely-oriented magnetization. First of all, the domain wall create a bound state split from the 2D continuum. Secondly, the band structure of the Rashba-effect surface has a nontrivial Berry curvature, thereby resulting in origination of the 1D resonant state with quasi-linear dispersion within the local exchange gap on the domain wall. Thirdly, in case of a relatively wide interdomain boundary the exchange gap can produce the resonant states with a parabolic spectrum. The main properties of the aforesaid states are described. In the final part of the article we discuss a possible role of the DW-induced electron states in the magnetotransport phenomena on the surface of the diluted REMS, for example, $\text{Bi}_{1-x}(\text{V},\text{Mn})_x\text{TeI}$.

2. Main part

In the diluted REMS, the moments that are localized on the magnetic atoms form the ferromagnetic order in a sample volume and/or in its surface area. Taking into account violation of both inversion symmetry near the surface of

the three-dimensional (3D) semiconductor and symmetry relative to time inversion, we describe the electron with the momentum $\mathbf{k} = (k_x, k_y)$, which moves along the surface, by means of an effective 2D Hamiltonian [32–34]

$$H(\mathbf{k}) = \frac{k^2}{2m^*} \sigma_0 - \alpha([\mathbf{k} \times \boldsymbol{\sigma}] \cdot \mathbf{e}_z) + JM(x, y)\sigma_z, \quad (1)$$

where $\boldsymbol{\sigma} = (\sigma_x, \sigma_y, \sigma_z)$ is the vector of the Pauli matrix, σ_0 is the identity 2×2 -matrix, $k = \sqrt{k_x^2 + k_y^2}$, m^* is the effective mass of the carriers in the surface area, α is the Rashba parameter. Hereinafter, a system of units where $\hbar = 1$ is used, unless specified otherwise. We omit summands that are higher than the second order in \mathbf{k} in the expansion of (1) around a center of the Brillouin zone $\bar{\Gamma}$. The last summand in (1) describes a relation of the electron spin and magnetization $\mathbf{M} = M\mathbf{e}_z$ via the exchange integral J , where \mathbf{e}_z is a normal to the surface. Since we are talking about the diluted magnetic semiconductor, then it is assumed that distribution of magnetization $M(x, y)$ along the surface, which is included in (1), is a result of averaging on a scale that exceeds an average distance between atoms of the magnetic impurity. For certainty, we consider the 2D electron states, which were formed near a bottom of the 3D conduction band of the semiconductor, although it is possible to similarly consider the 2D hole state near a top of the 3D valence band.

We remind that the spin-momentum coupling, which is implied in the second summand of the Hamiltonian (1), results in splitting the 2D spectrum into two parabolic bands with opposite spin polarization even without the magnetic order. In case of nontrivial homogeneous magnetization, $M(x, y) = M_0 = \text{const}$, the surface state become gapped states in the $\bar{\Gamma}$ point, obeying a dispersion relationship $E^{(\pm)}(k) = k^2/2m^* \pm \sqrt{\Delta_0^2 + \alpha^2 k^2}$, where $2\Delta_0 = 2JM_0$. At the same time the Berry curvature in the model (1) takes the form $\Omega^{(\pm)}(k) = \mp\alpha^2\Delta_0/(2[\Delta_0^2 + \alpha^2 k^2]^{3/2})$ [6,7], where $\Omega^{(+)}(k)/\Omega^{(-)}(k)$ is related to an upper/lower energy branch $E^{(+)}(k)/E^{(-)}(k)$, respectively. Using a standard definition for the Chern number as $C = \int d^2\mathbf{k}\Omega(k)/2\pi$ [6,7], it is possible to obtain the analytical dependence $C(\mu)$ on the Fermi level position μ [31]. At the same time, according to [31], the value of the this integral topological characteristic is essentially determined by the dimensionless parameter $|\Delta_0|/E_{so}$, where $E_{so} = m^*\alpha^2/2$ is the Rashba splitting energy, and its sign directly correlates with the direction of magnetization. The attention should be paid to the behaviour of the magnitude $C(\mu)$ within the energy area of the exchange gap when $\Delta_0^2 > \mu^2$. For example, if $E_{so} \ll |\Delta_0|$, then the Chern number becomes a vanishingly small quantity, $C(\mu) \approx E_{so}/\Delta_0$. In the opposite case, when the exchange splitting is comparatively weak, $E_{so} \gg |\Delta_0|$, the topological index approaches a half-integer value, $C(\mu) \approx [1 - (|\Delta_0|/4E_{so})] \text{ sign}(\Delta_0)/2$. Outside the exchange gap, i.e., when $\mu^2 > \Delta_0^2$, the magnitude $C(\mu)$ drastically decreases.

Now we analyze the situation with the solitary domain wall. We assume that the exchange field $\Delta(x, y) = \Delta(x)$ continuously increases with the coordinate x to go out to the asymptote $\Delta(x) \rightarrow \pm\Delta_0$, when $(x/\xi) \rightarrow \pm\infty$, where ξ is a characteristic scale of variation of the function $\Delta(x)$. Then, for certainty we assume that $\Delta_0 > 0$ and the domain wall is fixed along the line $x = 0$, i.e., $\Delta(x = 0, y) = 0$. A pair of semi-infinite ferromagnetic domains that differ from each other in the magnetization sign can be characterized by the local Chern numbers: the positive one for the right domain, $C_r > 0$ when $x > 0$, and the negative one for the left domain, $C_l < 0$ when $x < 0$. Thus, if the Fermi level is fixed inside the exchange gap, $|\mu| < \Delta_0$ and the condition $E_{so} \gg \Delta_0$ is fulfilled, then the topological index experiences a near-unit (almost quantized) change when transiting through the domain wall: $C_r - C_l \approx 1 - (\Delta_0/4E_{so})$. According to the correspondence principle [35,36], this situation can be interpreted as close critical regarding the appearance of the 1D electron state with particular properties at the boundary $x = 0$.

If neglecting the term quadratic in momentum in (1), it is possible to obtain an exact solution of the 1D problem $H(x, k_y)\theta(x, k_y) = \varepsilon(k_y)\theta(x, k_y)$ for the particular state, which energy linearly depends on the momentum, $\varepsilon^{(0)}(k_y) = \alpha k_y$, intersecting the exchange gap in the 2D spectrum $E_0^{(\pm)}(k) = \pm\sqrt{\Delta_0^2 + \alpha^2 k^2}$ [2]. The corresponding envelope wave function that is localized on the domain wall can be represented as $\theta^{(0)}(x) = \theta_0 \exp[-\alpha^{-1} \int_0^x \Delta(\xi) d\xi]$. The spectrum and spin polarization of this state do not depend on a specific distribution of the exchange field $\Delta(x)$, but are determined by an asymptotic limitation only, $\Delta(x \rightarrow \infty)\Delta(x \rightarrow -\infty) < 0$. I.e., the ground state is topologically protected. Indeed, if formally directing $m^* \rightarrow \infty$, we obtain $C_r - C_l = 1$. The state $\theta^{(0)}(x)$ is chiral: the direction of its spin polarization along the axis \mathbf{e}_x is strictly orthogonal to a direction of propagation of electron excitation along the domain wall. In addition to the topologically protected state, the domain wall can induce 1D trivial Volkov-Pankratov states (V-P) [37]. Their appearance depends on a ratio of a localization scale of the ground state $\propto \alpha/\Delta_0$ and the domain wall width $\propto \xi$. If the former exceeds the latter, $(\Delta_0\xi/\alpha) \ll 1$, then the gap has only the state $\varepsilon^{(0)}(k_y)$, whose spatial behavior can be approximated by the dependence $\theta^{(0)}(x) \sim \exp(-\Delta_0|x|/\alpha)$ that is typical for $\Delta(x) = \Delta_0 \text{sign}(x)$. Otherwise, $(\Delta_0\xi/\alpha) \gg 1$, the exchange gap hosts the energy branches with the spectrum $\varepsilon^{(\pm n)}(k_y) = \pm\sqrt{[\varepsilon^{(\pm n)}(0)]^2 + \alpha^2 k_y^2}$, $n = 1, 2, 3, \dots$, where $|\varepsilon^{(\pm n)}(0)| < \Delta_0$. The wider the domain wall, the larger the number of the states $\varepsilon^{(\pm n)}(k_y)$ with $n > 0$, which is induced by it within the exchange gap.

Inclusion of the quadratic summand into (1) results in certain modification of the above-described states. Near the $\bar{\Gamma}$, where the kinetic summand, $\propto k^2/2m^*$, is comparatively small, this problem was solved in principle for the low-energy state in the study [30]. It was shown that

scattering of electrons on an extremely narrow antiphase boundary of the type $\sigma_z \Delta_0 \text{sign}(x)$ (when $\xi = 0$) leads to the appearance of the 1D resonant state in the region of the local exchange gap on the surface of the semiconductor with the strong Rashba effect. In the approximation $\Delta_0 \ll 4E_{so}$ and $|k_y| \ll k_{so}$, where $k_{so} = \alpha m^*$, the dispersion relationship for this state can be explicitly obtained: $\varepsilon_R^{(0)}(k_y) = \alpha k_y + \omega_R^{(0)} - i\Gamma_R^{(0)}$ [30]. Thus, modification of the energy of the state $\varepsilon_R^{(0)}(k_y)$ consists in a small shift $\omega_R^{(0)} = \Delta_0^2/4E_{so}$ and spectral broadening $\Gamma_R^{(0)} = \Delta_0^3/8E_{so}^2$. The resonant state is quasi-bound. In addition to the component that is localized near the domain wall, its envelope function, $\theta_R^{(0)}(x, k_y) = \theta^{(0)}(x) + \vartheta(x, k_y)$, obtains an oscillating component, for which the following estimate is true $\vartheta(x, k_y = 0) \sim \vartheta_{\pm} \exp(\pm 2ik_{so}x)$. The weak spectral broadening, $\Gamma_R^{(0)} \ll \Delta_0$, and a low-amplitude correction to the envelope, $|\vartheta_{\pm}| \ll |\theta_0|$, is a result of overlapping of the energy of the 1D state $\varepsilon_R^{(0)}(k_y)$ with the lower branch of the 2D states $E^{(-)}(k)$ [30]. The resonant state is strongly (with accuracy to terms of the order of $(\Delta_0/E_{so})^2$) spin-polarized along the axis \mathbf{e}_x . On the other hand, with increase of the ratio Δ_0/E_{so} the spectral branch of the resonant state $\varepsilon_R^{(0)}(k_y)$ is smeared and its envelope $\theta_R^{(0)}(x, k_y)$ is delocalized. Finally, when $E_{so} \ll \Delta_0$, the 2D states lose the topological signs and, consequently, the features of the 1D resonant state in the real and momentum spaces disappear [30].

In order to clarify evolution of the 1D states emergent at the finite-width domain wall, we resorted to numerical analysis within the framework of the tight-binding approximation, performing lattice regularization of the Hamiltonian (1). Figure 1 schematically illustrates smooth variation of magnetization near the domain wall that induces the 1D resonant state. Without losing generality of the analysis, a spatial distribution of the exchange field was approximated by the function $\Delta(x) = \Delta_0 \tanh(x/\xi)$. By imposing periodic boundary conditions, we have calculated a single-particle spectral function. This procedure is described in more detail in the study [30]. Results of calculations of the spectral

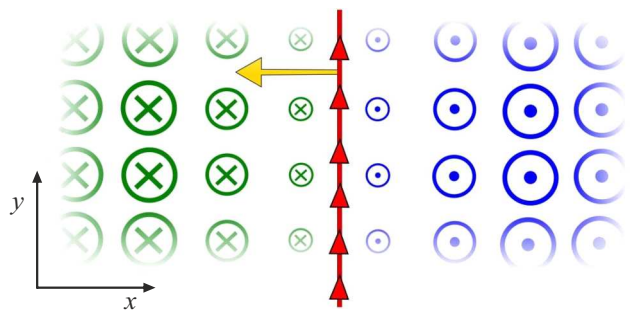


Figure 1. Schematic illustration of emergence of the 1D resonant state on the solitary domain wall on the REMS surface. The blue and green circles show variation of the amplitude and the sign of magnetization $\mathbf{M}(x) = M(x)\mathbf{e}_z$ near the domain wall on the REMS surface. The red line symbolizes a unidirectional nature of the resonant state, while the yellow arrow marks a direction of its spin polarization.

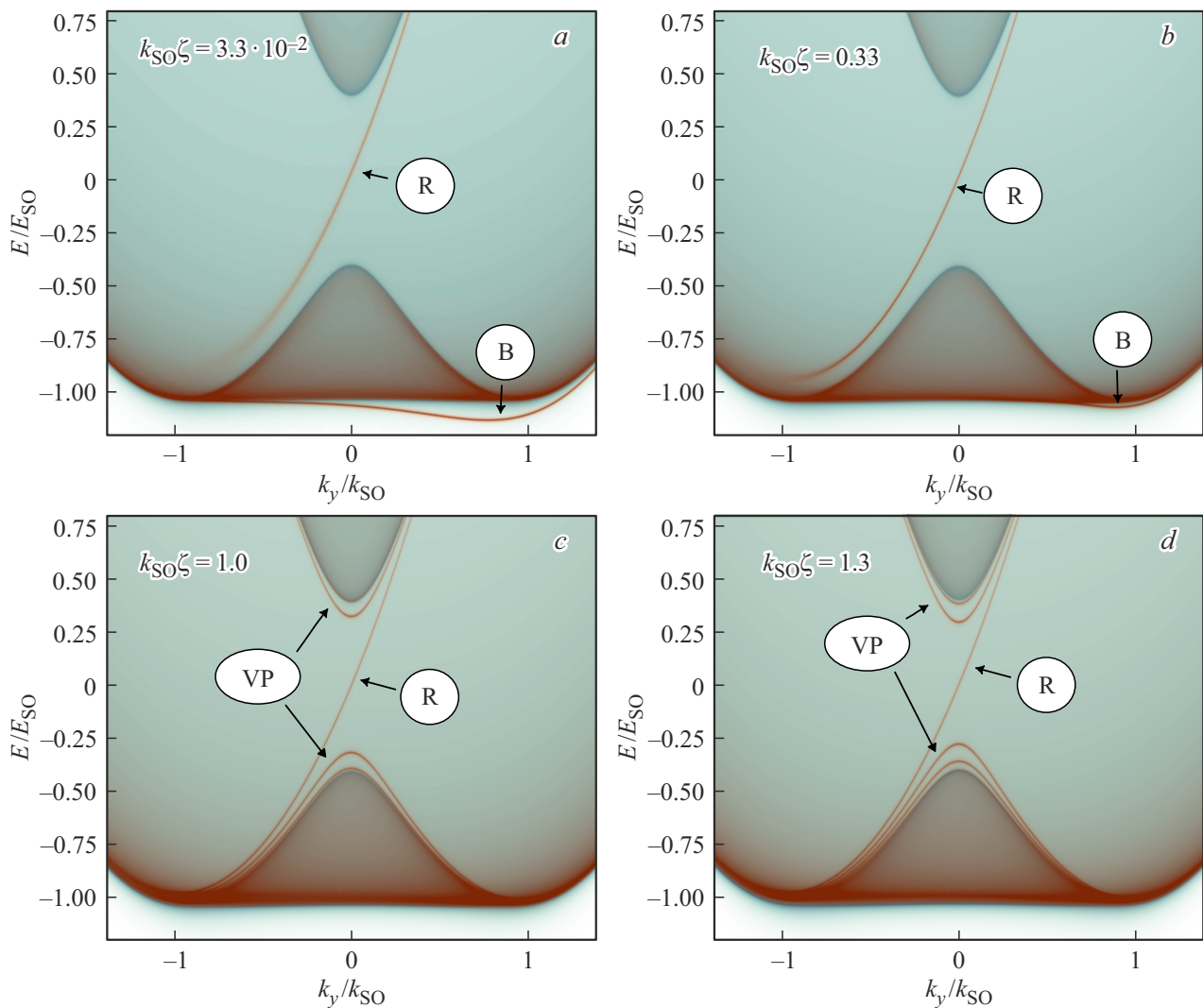


Figure 2. Evolution of the spectral characteristics of the 1D electron states on the REMS surface, which are induced by the solitary amplitude domain wall, with increase of its width ζ . The distribution of the exchange field is defined as $\Delta(x) = \Delta_0 \tanh(x/\zeta)$. The four panels (a), (b), (c), (d) correspond to key moments of variation of dispersion of the 1D states. Each panel reflects intensity of the spectral function for the wall, with increase of its width ζ . The distribution of the given dimensionless parameter $k_{so}\zeta$. A ratio of the exchange splitting energy to the Rashba splitting energy is given by the value ($\Delta_0/E_{so} = 0.4$). The spectral functions of the 1D states are represented by thin cherry-color lines against the background of projection of the spectral function of the 2D states in the magnetic domains, $E^{(\pm)}(k)$. The symbols R, VP and B denote the gapless resonant state, $\varepsilon_R^{(0)}(k_y)$, the Volkov-Pankratov resonant states, $\varepsilon_R^{(\pm n)}(k_y)$ with $n > 0$ and the bound state, $\varepsilon_B(k_y)$, respectively.

behavior of the surface states in the situation of the relatively weak exchange field $\frac{\Delta_0}{E_{so}} = 0.4$ are shown in Figure 2. Four qualitatively different cases are selected: (a) an extremely hard domain wall, when $k_{so}\zeta \ll 1$; (b) a moderately hard domain wall, when $k_{so}\zeta < 1$; (c) an intermediate-width domain wall, $k_{so}\zeta \approx 1$; (d) a soft domain wall, $k_{so}\zeta > 1$. It is easy to distinguish the 2D surface states in the domains from the 1D resonant states on the domain wall. The branch with quasi-linear dispersion $\varepsilon_R^{(0)}(k_y)$ is located between projections of the bands $E^{(\pm)}(k)$. It is noteworthy that the only essential change in the behavior of the gapless state with variation of the domain wall width, which can be noted in Figure 2, is a narrowing of the spectral broadening of $\Gamma_R^{(0)}$

with increase of the magnitude of $k_{so}\zeta$. Rough assessment provides a two-fold decrease of the value of $\Gamma_R^{(0)}$ at $k_y = 0$, when the parameter $k_{so}\zeta$ increases from 0 to 1.3 (Figure 2). The effect of the domain wall texture on spectral broadening of the resonant state $\varepsilon_R^{(0)}(k_y)$ is explained at a qualitative level by the fact that in case of the finite-width domain wall the electron that is localized on the scale of the envelope function $\theta_R^{(0)}(x, k_y)$ is affected by the smaller-value exchange field as compared to Δ_0 . Figure 3 demonstrates that the gapless resonant state exhibits a chirality property: it is highly-spin-polarized along the axis \mathbf{e}_x , which is orthogonal both to the domain wall direction \mathbf{e}_y and to orientation of magnetization in the domains $\pm \mathbf{e}_z$.

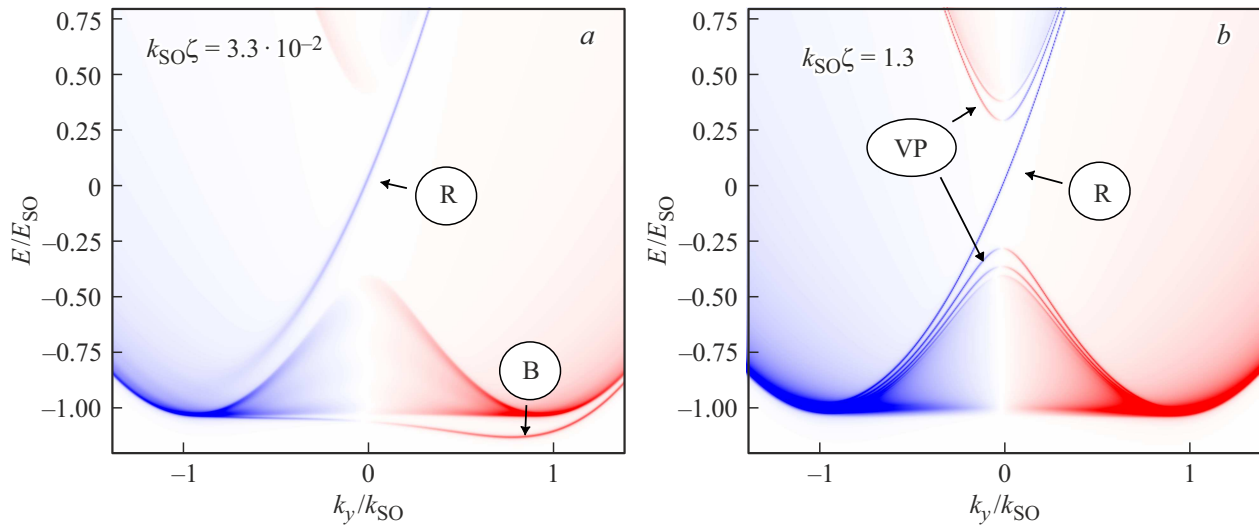


Figure 3. Spin polarization of the 1D electron states on the REMS surface, which are induced by the single amplitude domain wall. The panels reflect intensity of the spectral function with taking into account spin resolution for the two different values of the dimensionless parameter $k_{so}\zeta$. A ratio of the exchange splitting energy to the Rashba splitting energy is defined by the value $(\Delta_0/E_{so}) = 0.4$. Positive/negative polarization along the axis \mathbf{e}_x is shown by the blue/red color. The symbols R, VP and B denote the gapless resonant state, $\varepsilon_R^{(0)}(k_y)$, the Volkov-Pankratov resonant states, $\varepsilon_R^{(\pm n)}(k_y)$ with $n > 0$ and the bound state, $\varepsilon_B(k_y)$, respectively.

We note that when inverting the direction of magnetization in the studied system, or, in other words, when formally replacing $\Delta(x)$ with $-\Delta(x)$, the 1D gapless state $\varepsilon_R^{(0)}(k_y)$ changes the signs of the speed and spin polarization.

At the domain wall, there is also the bound state $\varepsilon_B(k_y)$, which is located below the 2D band. The effective potential that is proportional to the value of the exchange field gradient, $|\partial\Delta(x)/\partial x|$, splits the bound state $\varepsilon_B(k_y)$ from a lower edge of the branch $E^{(-)}(k)$. As can be seen in Figure 2, as the domain wall width increases, in other words, with decrease of the gradient value, the energy branch $\varepsilon_B(k_y)$ is pressed against the line segment $|k_y| \leq \sqrt{k_{so}^2 - (\Delta_0/\alpha)^2}$ that connects the minimums of the lower 2D band.

In case of the comparatively narrow domain wall that is represented by the panels (a) and (b) in Figure 2, the interval of the local exchange gap, $|E| < \Delta_0$, hosts the resonant state $\varepsilon_R^{(0)}(k_y)$ only. In case of the intermediate-width domain wall, $k_{so}\zeta \approx 1$, as can be seen in the panel (c), a pair of the V-P-type states originates [37], with one state at an upper and a lower edge of the exchange gap, $\varepsilon_R^{(\pm 1)}(k_y)$. In case of the comparatively wide domain wall, as exemplified by the panel (d), the gap hosts the states $\varepsilon_R^{(\pm n)}(k_y)$ with $n > 1$. The extremely wide domain wall ($k_{so}\zeta \gg 1$) generates multiple V-P-type states that densely fill the entire exchange gap. As can be seen from the figure, the V-P-type states $\varepsilon_R^{(\pm n)}(k_y)$ are also resonant states, wherein they have a noticeably larger spectral broadening $\Gamma_R^{(\pm n)}$ as compared to $\Gamma_R^{(0)}$. Spin polarization of the 1D V-P states clearly correlates with polarization of a projection of the 2D state, from which they originate (Figure 3). It should be noted that although the resonant V-P-type states are not directly related to the

topological specific features of the 2D REMS spectrum, they necessarily appear (along with the gapless resonant state) on the quite wide domain wall, $k_{so}\zeta > 1$.

3. Discussion and conclusion

Above, we have described the spectral properties of the REMS surface that includes the finite-width domain wall. Certainly, among the 1D states induced by the domain wall, the most interesting is the gapless resonant state with a spin density orthogonal to the domain wall. According to the estimates done in the studies [29,30], for the case of the hard domain wall a suitable platform for experimental detection of such a state can be the diluted REMS $\text{Bi}_{1-x}(\text{V,Mn})_x\text{TeI}$ [27–29]. The Van der Waals semiconductor material BiTeI has a volume band gap ~ 0.38 eV, which includes the 2D Rashba state with a record high value of the parameter $\alpha = 3.85$ meV \cdot Å and splitting $E_{so} \approx 0.1$ meV on the surface that is formed by the Te atoms [24]. Doping BiTeI with the V or Mn atoms of the concentration x from 2 to 3 % results in opening of the exchange gap $2\Delta_0$ of up to one hundred of meV in the $\bar{\Gamma}$ point due to surface ferromagnetic ordering of the local moments along the easy axis \mathbf{e}_z with the relatively high Curie temperature $T_C \approx 130$ K [27–29]. It should be expected that the boundary between the ferromagnetic domains with transverse magnetization at the Te surface of $\text{Bi}_{1-x}(\text{V,Mn})_x\text{TeI}$ is a source of long-lived spin-polarized resonance with the quasi-linear spectrum $\sim \pm \alpha k_y$ and the lifetime $\tau_R^{(0)}$. The magnitude $\tau_R^{(0)} = [\Gamma_R^{(0)}]^{-1}$ is determined by the typical time interval, during which the density of probability of excitation, $|\theta_R^{(0)}(x, k_y)|^2$, which moves along

the domain wall in a ballistic mode, flows into into the 2D state $E^{(-)}(k)$. As shown above, spectral broadening $\Gamma_R^{(0)}$ somewhat decreases with increase of the domain wall width ς . I.e., the resonant state $\varepsilon_R^{(0)}(k_y)$ becomes more stable in the sense of increase of the lifetime $\tau_R^{(0)}$. However, on the other hand, the quite wide domain wall generates the resonant V-P-type states $\varepsilon_R^{(n)}(k_y)$ that will shunt a contribution of the resonant state $\varepsilon_R^{(0)}(k_y)$ into the transport and magnetotransport phenomena, when the Fermi level μ is outside the energy interval $\varepsilon_R^{(-1)}(0) < \mu < \varepsilon_R^{(1)}(0)$. And with increase of ς this interval narrows. It is obvious that the similar issue will arise when trying to observe the state $\varepsilon_R^{(0)}(k_y)$ by means of scanning tunnel spectroscopy.

In the present study, we have investigated origination of the 1D electron states at the magnetic domain wall at the REMS surface and their modification with variation of the domain wall width. It is shown that the gapless resonant state that should be interpreted as a marker of the nontrivial Berry curvature of the 2D states, not only maintains quasi-linear dispersion and spin polarization, but becomes more stable with increase of the domain wall width as well. Besides, the domain wall can induce the trivial states, namely: the bound state and the resonant Volkov-Pankratov-type state, whose behavior depends on the domain wall width. Thus, it is reasonable to expand the scope of the systems that combine magnetic ordering and specific features of the band structure over the magnetic semiconductors with the strong Rashba effect and to focus attention on searching low-dissipative electron states on the boundaries of the various magnetic phases in these materials.

Funding

The present study was financially supported by St. Petersburg State University, project No. 125022702939-2.

Conflict of interest

The authors declare that they have no conflict of interest.

References

- [1] C.-Z. Chang, C.-X. Liu, A.H. MacDonald. Rev. Mod. Phys. **95**, 1, 011002 (2023).
- [2] Y. Tokura, K. Yasuda, A. Tsukazaki. Nature Reviews Physics **1**, 1, 126 (2019).
- [3] M.M. Otrokov, T.V. Menshchikova, M.G. Vergniory, I.P. Rusinov, A.Yu. Vyazovskaya, Yu.M. Koroteev, G. Bihlmayer, A. Ernst, P.M. Echenique, A. Arnaud, E.V. Chulkov. 2D Materials **4**, 2, 025082, (2017).
- [4] Y. Zhao, Q. Liu. Appl. Phys. Lett. **119**, 6, 060502 (2021).
- [5] J.-X. Qiu, B. Ghosh, J. Schütte-Engel, T. Qian, M. Smith, Y.-T. Yao, J. Ahn, Y.-F. Liu, A. Gao, Ch. Tzsaschel, H. Li, I. Petrides, D. Bérubé, T. Dinh, T. Huang, O. Lieberman, E.M. Been, J.M. Blawat, K. Watanabe, T. Taniguchi, K.C. Fong, H. Lin, P.P. Orth, P. Narang, C. Felser, T.-R. Chang, R. McDonald, R.J. McQueeney, A. Bansil, I. Martin, N. Ni, Q. Ma, D.J.E. Marsh, A. Vishwanath & Su-Yang Xu. Nature **641**, 5, 62 (2025).
- [6] D. Xiao, M.C. Chang, & Q. Niu. Rev. Mod. Phys. **82**, 3, 1959 (2010).
- [7] N. Nagaosa, J. Sinova, S. Onoda, A.H. MacDonald, & N.P. Ong. Rev. Mod. Phys. **82**, 2, 1539 (2010).
- [8] J.G. Checkelsky, J.T. Ye, Y. Onose, Y. Iwasa, & Y. Tokura. Nat. Phys. **8**, 10, 729 (2012).
- [9] I.T. Rosen, E.J. Fox, X. Kou, L. Pan, Kang L. Wang, D. Goldhaber-Gordon. Quantum Materials **2**, 12, 69 (2017).
- [10] Y. Shi, Y. Bai, Y. Li, Y. Feng, Q. Li, H. Zhang, Y. Chen, Y. Tong, J. Luan, R. Liu, P. Ji, Z. Gao, H. Guo, J. Zhang, Y. Wang, X. Feng, K. He, X. Zhou, J. Shen. Phys. Rev. Materials **8**, 12, 124202 (2024).
- [11] Y.-F. Zhao, R. Zhang, J. Cai, D. Zhuo, L.-J. Zhou, Z.-J. Yan, M. H. W. Chan, X. Xu & C.-Z. Chang. Nature Communications, **14**, 1, 770 (2023).
- [12] M. Allen, Y. Cui, M.E. Yue, M. Mogi, M. Kawamura, I.C. Fulga, D. Goldhaber-Gordon, Y. Tokura, Z.-X. Shen. Proc. Natl Acad. Sci. USA, **116**, 29, 14511 (2019).
- [13] R. Wakatsuki, M. Ezawa, N. Nagaosa. Sci. Rep. **5**, 9, 13638 (2015).
- [14] P. Upadhyaya, Y. Tserkovnyak. Phys. Rev. B **94**, 2, 020411(R) (2016).
- [15] Y. Ferreiros, F.J. Buijnsters, M.I. Katsnelson. Phys. Rev. B **92**, 8, 085416 (2015).
- [16] V.N. Men'shov, E.V. Chulkov. JETP Lett. **117**, 2, 147 (2023).
- [17] V.N. Men'shov, I.A. Shvets, E.V. Chulkov. JETP Lett. **110**, 12, 771 (2019).
- [18] V.N. Men'shov, I.A. Shvets, E.V. Chulkov. Phys. Rev. B **106**, 20, 205301 (2022).
- [19] I.P. Rusinov, V.N. Men'shov, E.V. Chulkov. Phys. Rev. B **104**, 3, 035411 (2021).
- [20] V.N. Men'shov, I.P. Rusinov, E.V. Chulkov. JETP Lett. **114**, 11, 699 (2021).
- [21] V.N. Men'shov, I.A. Shvets, E.V. Chulkov. Phys. Rev. B **99**, 11, 115301 (2019).
- [22] E.K. Petrov, V.N. Men'shov, I.P. Rusinov, M. Hoffmann, A. Ernst, M.M. Otrokov, V.K. Dugaev, T.V. Menshchikova, E.V. Chulkov. Phys. Rev. B **103**, 23, 235142 (2021).
- [23] N.P. Armitage, E.J. Mele, A. Vishwanath. Rev. Mod. Phys. **90**, 1, 015001 (2018).
- [24] K. Ishizaka, M.S. Bahramy, H. Murakawa, M. Sakano, T. Shimojima, T. Sonobe, K. Koizumi, S. Shin, H. Miyahara, A. Kimura, K. Miyamoto, T. Okuda, H. Namatame, M. Taniguchi, R. Arita, N. Nagaosa, K. Kobayashi, Y. Murakami, R. Kumai, Y. Kaneko, Y. Onose and Y. Tokura. Nature Materials **10**, 6, 521 (2011).
- [25] S.V. Eremeev, I.A. Nechaev, Yu.M. Koroteev, P.M. Echenique, E.V. Chulkov. Phys. Rev. Lett., **108**, 24, 246802 (2012).
- [26] G. Landolt, S.V. Eremeev, Yu.M. Koroteev, B. Slomski, S. Muff, M. Kobayashi, V.N. Strocov, T. Scmitt, Z.S. Aliev, M.B. Babanly, I.R. Amiraslanov, E.V. Chulkov, J. Osterwalder, J.H. Dil. Phys. Rev. Lett. **109**, 11, 116403 (2012).
- [27] I.I. Klimovskikh, A.M. Shikin, M.M. Otrokov, A. Ernst, I.P. Rusinov, O.E. Tereshchenko, V.A. Golyashov, J. Sánchez-Barriga, A.Yu. Varykhalov, O. Rader, K.A. Kokh, E.V. Chulkov. Scientific Reports **7**, 6, 3353 (2017).
- [28] A.M. Shikin, A.A. Rybkina, I.I. Klimovskikh, O.E. Tereshchenko, A.S. Bogomyakov, K.A. Kokh, A. Kimura, P.N. Skirkov, K.A. Zvezdin, A.K. Zvezdin. 2D Mater. **4**, 2, 025055 (2017).

- [29] A.M. Shikin, A.A. Rybkina, D.A. Estyunin, I.I. Klimovskikh, A.G. Rybkin, S.O. Filnov, A.V. Koroleva, E.V. Shevchenko, M.V. Likholetova, V.Yu. Voroshnin, A.E. Petukhov, K.A. Kokh, O.E. Tereshchenko, L. Petaccia, G. Di Santo, S. Kumar, A. Kimura, P.N. Skirdkov, K.A. Zvezdin, A.K. Zvezdin. *Scientific Reports* **11**, 12, 23332 (2021).
- [30] I.P. Rusinov, V.N. Men'shov, E.V. Chulkov. *Phys. Rev. B* **110**, 19, 195405 (2024).
- [31] V.N. Men'shov, I.P. Rusinov, E.V. Chulkov. *JETP Lett.* **121**, 5, 372 (2025).
- [32] G. Bihlmayer, O. Rader, R. Winkler. *New J. Phys.* **17**, 5, 050202 (2015).
- [33] A. Manchon, H.C. Koo, J. Nitta, S.M. Frolov, R.A. Duine. *Nature Materials* **14**, 9, 871 (2015).
- [34] G. Bihlmayer, P. Noël, D.V. Vyalikh, E.V. Chulkov, A. Manchon. *Nature Reviews Physics* **4**, 8, 642 (2022).
- [35] M.Z. Hasan, C.L. Kane. *Rev. Mod. Phys.* **82**, 4, 3045 (2010).
- [36] X.L. Qi, S.C. Zhang. *Rev. Mod. Phys.* **83**, 4, 1057 (2011).
- [37] B.A. Volkov, O.A. Pankratov. *JETP Lett.* **42**, 4, 178 (1985).

Translated by M.Shevlev